

PAPER

CO-tip manipulation using repulsive interactions

To cite this article: Nana K M Nazriq *et al* 2018 *Nanotechnology* **29** 495701

View the [article online](#) for updates and enhancements.



IOP | ebooks™

Bringing you innovative digital publishing with leading voices to create your essential collection of books in STEM research.

Start exploring the [collection](#) - download the first chapter of every title for free.

CO-tip manipulation using repulsive interactions

Nana K M Nazriq¹, E Minamitani² and T K Yamada^{1,3,4} 

¹ Department of Materials Science, Chiba University, 1-33 Yayoi-cho, Inage-ku, Chiba 263-8522, Japan

² Department of Materials Engineering, The University of Tokyo, Bunkyo-ku, Tokyo 113-8656, Japan

³ Molecular Chirality Research Center, Chiba University, 1-33 Yayoi-cho, Inage-ku, Chiba 263-8522, Japan

E-mail: toyoyamada@faculty.chiba-u.jp

Received 20 June 2018, revised 7 September 2018

Accepted for publication 12 September 2018

Published 4 October 2018



CrossMark

Abstract

Understanding the interactions between a tip apex and a target atom or molecule is crucial for the manipulation of individual molecules with precise control by using scanning tunnelling microscopy (STM) and atomic force microscopy. Herein, we demonstrate the manipulation of target CO molecules on a Cu(111) substrate using a CO-functionalized W tip with atomic-scale accuracy. All experiments were performed in a home-built ultra-high vacuum STM system at 5 K. The CO-tip was fabricated by picking up a single CO molecule from a Cu(111) surface. In contrast to a metal tip, repulsive interactions occur between the CO-tip and the target CO molecule. This repulsive interaction promises perfect lateral hopping without any vertical hopping. Hopping events were directly monitored as sudden current drops in the simultaneously measured I - z curves. A larger barrier height between the CO-tip and the target CO (~ 9.5 eV) was found from the slope of the I - z curve, which decreases the electron tunnelling probability between the tip and sample. Therefore, electron-driven manipulation cannot be a major trigger for the CO-CO repulsive manipulation. The CO-tip is able to manipulate only the target CO molecule, even when another CO molecule was located ~ 0.5 nm away. Statistical measurements revealed that the nearest neighbour atop site is the energetically stable position after hopping. However, if the CO target has another CO molecule in a neighbouring position (denoted as a 'pair'), the target CO hops more than twice as far. This means that the CO-tip experiences a larger repulsive interaction from the pair. These observations of CO-tip manipulation are useful for the design of two-dimensional artificial molecular networks as well as for developing a better understanding of catalytic oxidation processes.

Supplementary material for this article is available [online](#)

Keywords: carbon mono oxide, manipulation, STM, molecule functionalized tip, repulsive interaction

(Some figures may appear in colour only in the online journal)

Introduction

Manipulation techniques using probe microscopy, namely scanning tunnelling microscopy (STM) and atomic force microscopy (AFM) can enable the fabrication of artificial nanostructures on a substrate by assembling atoms and molecules using *in situ* observations [1–4]. Such techniques

have attracted significant attention as a powerful tool for developing next-generation 1 nm sized devices and for studying fundamental single-atom-size physical phenomena.

Various substrates, such as metals, semiconductors, and insulators, have been tested as a *playground* for the manipulation of single atoms or molecules, whereas metal tips have been mostly used for the manipulation. The interaction (either attractive and/or repulsive) between a metal atom at the tip apex and the adsorbed target leads to not only lateral hopping

⁴ Author to whom any correspondence should be addressed.

on the substrates, but also vertical manipulation at the tip apex [5, 6]. In addition to these simple interactions, molecular vibrations excited via electron injection from the probe tip have also been utilised for molecular manipulation [1–3]. A series of previous investigations on CO molecules adsorbed on metal surfaces have served as a model system to reveal the elementary steps in catalytic oxidation [7–9]. More recently, CO molecules adsorbed on metal surfaces have attracted attention as building blocks for molecular logic gates or artificial two-dimensional networks [2, 3, 10–12]. CO molecules have been not only the target of observation, but they have also been used to functionalise probe tips [5, 13, 14]. CO-functionalised tips have attracted significant attention because they enable extremely high spatial resolution [15]. Such high-resolution imaging is possible with a CO-tip because of the Pauli repulsion between the closed shell molecule on the probe and the electronic charge of the adsorbed molecule being probed. In addition, it is expected that the force field from the CO tip would be different from that reported in the case of a bare W tip [5, 13]. Accordingly, molecular force interactions between the CO tip and a CO molecule on the substrate have been investigated using AFM [14, 16–20], suggesting that the repulsive interaction tilts the CO molecule axes standing perpendicular to the metal substrate and tip. This indicates that the force field from the CO tip can be applied for molecular manipulation; however, this possibility has never been demonstrated.

In this article, we demonstrate CO-tip manipulation using repulsive interaction between a CO molecule on a Cu(111) substrate and a CO-functionalised W tip. A home-built ultrahigh vacuum (UHV) cryogenic temperature (5 K) STM system was used. The gentle touching which results from the repulsive interaction between the CO-tip and the target CO molecule precludes breaking or picking up the target molecule. In contrast to bare metal tips, this CO tip promises perfect lateral hopping. Vertical hopping was never observed. We repeated the approach for the CO-tip to the CO molecules on the substrate and obtained statistical results showing that the closest atop site is the most energetically stable position after hopping. The CO-tip manipulation enables to hop a target molecule with atomic-scale accuracy. We directly monitored the CO-tip lateral manipulation by simultaneously measuring the I - z curve (tunnelling current as a function of tip-sample separation). A current drop always occurred when the target molecule hopped. From the slope of the I - z curve, the CO-tip was found to have a markedly large barrier height. The CO-tip manipulation was also performed for a CO-pair (two CO molecules sitting next each other at ~ 0.5 nm separation). The CO-tip successfully manipulated only one CO molecule in the pair. Statistical measurements for the pair showed that the hopping distance more than doubled, while the hopping event occurred at a shorter CO-tip displacement. The CO tip experiences a larger repulsive interaction from the pair than from the monomer.

CO-tip manipulation is useful for not only enhancing the spatial resolution of STM/AFM, but also for fabricating a two-dimensional CO molecular network or developing a better understanding of catalytic oxidation processes.

Results and discussion

All experiments were performed using a home-built UHV low-temperature STM setup (see supplementary information, figure S6, available online at stacks.iop.org/NANO/29/495701/mmedia). A CO-terminated tip was fabricated by picking up a single CO molecule on a Cu(111) surface at 5 K. An atomically-flat and clean Cu(111) surface was prepared inside the preparation chamber by repeated Ar⁺ sputtering and annealing cycles (see supplementary information, figure S5). Without breaking UHV, the Cu(111) substrate was set into the 5 K STM stage located inside the analytical UHV chamber. CO molecules were adsorbed inside the STM. A chemically etched W tip cleaned in the UHV preparation chamber via proper flashing was used [21]. We successfully manipulated CO molecules on Cu(111) using the W tips (see supplementary information, figure S5). Then, we confirmed that, because of attractive interactions between the W tip apex and the CO molecule, the W tip had a 50% chance of picking up a target CO molecule, thus producing a CO-tip. Voltage pulses have also been used to pick up CO molecules on a W tip [6, 14, 18, 19, 22], but here, simply a use of the attractive interaction is enough to produce a CO-tip. The single CO molecules on the metal substrate were observed in the STM images as dark spots by using the metal W tip; however, the STM images obtained using the CO tip showed bright protrusions with halo-like depressions (see supplementary information, figure S1).

Figure 1 shows a demonstration of STM vertical manipulation of a single CO molecule on Cu(111). In figure 1(a), thirteen molecules (Nos. 1–13) can be observed as dark spots when scanned with a clean W-tip. We recorded the STM image in figure 1(b) by starting the scan of figure 1(a) from the top with a clean W tip. When the W tips came to the molecule No. 2 position, the tip was made to approach the surface. Previous AFM and density functional theory (DFT) studies showed that attractive forces are dominant, which explains the jump of the CO molecule from the Cu(111) substrate to the W tip apex (vertical hopping) [16, 18, 19, 23–29]. Then, we restarted the scan. Molecule No. 2 could no longer be seen, while the observed contrast of molecules No. 3–13 changed. Now the molecules could be observed as bright protrusions with halo-shaped depressions. The line profiles (shown in supplementary information, figure S1) show that the protrusions have a height of 8.0 ± 2.0 pm and a diameter of 1.0 ± 0.2 nm. These observations provide clear indication that the tip now has a CO molecule at its apex.

Because of the attractive interaction between CO and metal surfaces, we can also return the CO molecule to the Cu(111) substrate from the W tip apex. We approached the tip near the lower left of molecule No. 7 and this caused molecule No. 2 (dotted circle) to be transferred back to the Cu(111) surface, leaving the tip as bare W again. Figure 1(c) shows this result, where the image is the same as that in figure 1(a) and the CO molecules can be observed as dark spots. Sphere models of the vertical manipulation process are shown in figure 1(d).

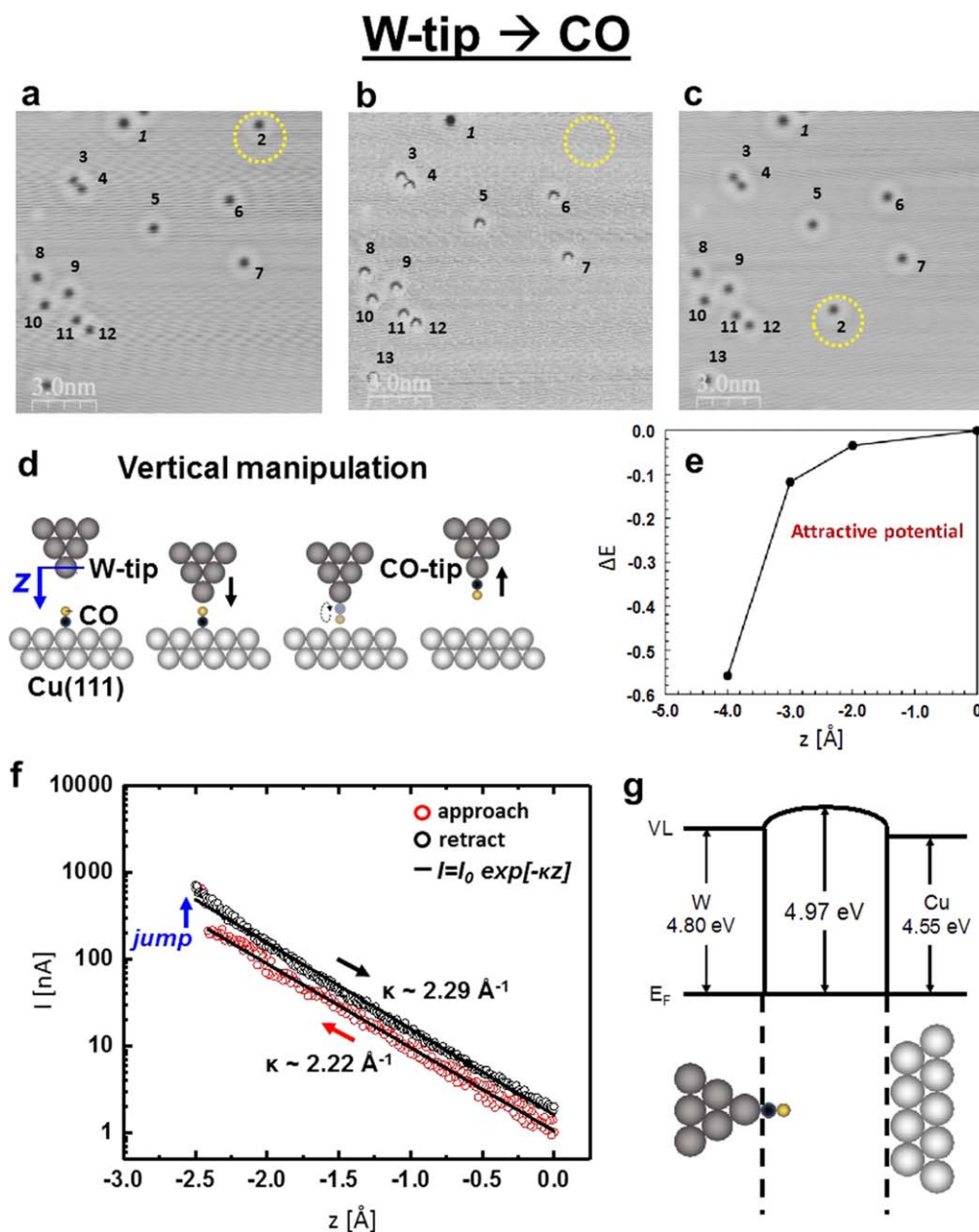


Figure 1. Fabrication of the CO-terminated W tip. (a) STM image scanned with a clean W tip. A total of 13 single molecules are observed as dark spots ($V_s = 0.47 \text{ V}$, $I = 0.7 \text{ nA}$). (b), (c) STM images obtained from the same area as (a) ($V_s = 0.47 \text{ V}$, $I = 0.7 \text{ nA}$). (b) The W tip picked up CO molecule No. 2; thus, the observed contrast changed for molecules No. 3-13. (c) Molecule No. 2 adsorbed on the W tip apex was dropped back onto the substrate, so this STM image was obtained with a bare W tip again. (d) Sphere models depicting the vertical manipulation process. (e) Total energy variation as a function of tip apex displacement obtained by DFT calculation. (f) I - z spectroscopy curve (on log scale) during the approach. The red circles show the approaching direction of the W-tip and the black circles correspond to the retracting direction of the tip with CO attached at the apex. Insets show schematic diagrams during the approaching process. The decay rate (κ) was obtained by the least squares fitting of $I = I_0 \exp[-\kappa z]$ to the experimentally obtained I - z data points: $\kappa = 2.220 \pm 0.013 \text{ \AA}^{-1}$ for approaching and $\kappa = 2.286 \pm 0.010 \text{ \AA}^{-1}$ for retracting. (g) Measured barrier height between the CO-tip and the Cu(111) substrate. Work function of Cu(111) (4.55 eV) and W(110) (4.80 eV) are shown [41]. E_F and VL denote the Fermi energy and vacuum level, respectively.

Such STM imaging with a CO-tip has also attracted much attention as a method for visualising the atomic-scale chemical structure of a single organic molecule [6, 18]. We tested the CO-tip for a single metal-free phthalocyanine molecule (H_2Pc) and observed extra structures which were not possible to observe with a bare W tip, i.e., a W tip showed only four bright spots, while the CO-tip showed two-fold symmetry in the molecule, referring to two H atoms at the

centre of H_2Pc . (see supplementary information, figures S1(g), (h))

Figure 1(f) shows I - z curves during the *pick-up* process. The primary vertical axis denotes the current detected by the tip (log scale) and the x -axis denotes the relative tip-sample distance. The conductance was calculated using the relationship $G = IV$ in units of the quantum conductance factor, $G_0 = 2e^2/h$. The initial position of the tip was set as $z = 0 \text{ pm}$

during the tunnelling feedback. The substrate bias was set to +50 mV. The W-tip approached the CO molecule from the initial position $z = 0$ Å. During the approach, the current increased exponentially owing to tunnelling electron transmission (red circles in figure 1(d); here shown in linear-log scale). However, at $z = -2.40$ Å, the conductance abruptly jumped from 200 to 600 nA. Then, the tip was retracted back to the original position (from $z = -2.40$ Å to $z = 0$ Å) (black circles in figure 1(f)). The I - z curves in figure 1(f) were successfully fitted to the function $I = I_0 \exp[-\kappa z]$ [30]. The barrier height, ϕ , between the tip and the sample was obtained from the decay rate, $\kappa = \sqrt{(32\pi^2 m\phi)/h}$, where m and h denote the electron mass and Planck's constant, respectively. The decay rates before and after the hopping were $\kappa \sim 2.22$ Å⁻¹ and $\kappa \sim 2.29$ Å⁻¹, respectively. The obtained barrier height between the W-tip and the CO/Cu(111) was 4.69 eV and the barrier height between the CO-tip and the Cu(111) was 4.97 eV (see figure 1(g)). Since both systems are symmetric, the barrier height was almost constant.

Further, the I - z measurements in figure 1(f) show the conductance through the CO single molecule to be $0.10 \pm 0.05 G_0$, which is in good agreement with previous STM conductance results [19].

The total energy of the metal-tip and the CO molecule adsorbed on Cu(111) was calculated as a function of the distance between the tip and the substrate (see figure 1(e)). Starting from the initial position ($z = 0$), the total energy decreased, indicating that attractive interactions dominate in this system, producing a jump of the CO from the Cu(111) substrate to the W-tip apex even without an applied voltage pulse.

CO-tip manipulation of CO-monomer

We fabricated a CO-tip by using the attractive interactions between the W tip and the CO molecule as shown in figure 1. Here, we demonstrated what happens when the CO tip approaches a target CO molecule on the substrate. Figure 2(a) shows an image of two single CO molecules on Cu(111) obtained by using the CO-tip. Hexagonal lines showing the fcc(111) atomic lattice, as obtained from an atomically resolved Cu(111) STM image (see the inset), are overlaid on this image as a visual guide. CO molecules on Cu(111) are located at the energetically stable atop site positions.

Now, the CO tip was approached toward the target CO molecule on Cu(111) (black circle in figure 2(a)). The tip apex was moved ~ 2 Å toward the molecule and then moved back to the initial position. Subsequently, the same area was scanned as that shown in figure 2(b). Again, two CO molecules were observed; however, it can be observed that the approached target CO molecule hopped approximately two times the atomic distance ($2d = 2a/\sqrt{2}$, where a denotes the lattice constant of fcc-Cu: 0.361 nm) along the [011] direction to a bridge site.

We repeated the same approaching process toward the same target molecule and obtained similar results. Only the approached target molecule moved. Consecutive STM images

shown in figures 2(a), (b) demonstrate that the CO tip is able to repulsively manipulate surface molecules with atomic-scale accuracy. The interactions between the CO tip and the CO molecule on the substrate during this approaching process can be investigated by simultaneous monitoring of the tunnelling current (I) as a function of the tip apex displacement (z). Figure 2(d) shows the obtained I - z curves.

When the tip started to move toward the target molecule from the initial position ($z = 0$ Å), the tunnelling current increased exponentially, $I \propto I_0 \exp[-\kappa(S_0 + z)]$, where κ , S_0 , and z denote the decay rate, initial tip-sample separation, and tip apex displacement, respectively (here plotted on a log scale). During the exponential increases, both CO molecules on the tip and substrate remain at their original positions. However, at approximately $z = -1.60 \pm 0.15$ Å, we observed a current drop (~ 40 nA down). Below $z < -1.65$ Å, the current increased exponentially again. By comparing our data with previous AFM results [14, 18, 19], both CO molecules on the tip and substrate could start to tilt before hopping when facing opposite to each other. It should be noted that the wavy noise in the I - z curves increased compared to figure 1(f); this increased noise could represent instability due to repulsive interactions between the CO-tip and the CO single molecules on the Cu(111) surface. Further moving the CO tip toward the CO target enhanced the repulsive force. When the repulsive force overcame the adsorption energy of the CO molecule on the substrate, lateral hopping occurred. The drop in the tunnelling current in figure 2(d) is a sign of lateral CO hopping. Since the I - z curve was measured under feedback-off conditions, if the molecule below the tip was suddenly moved, the tunnelling current decreased owing to an increase in the tip-sample separation based on the CO molecule height (ΔS), i.e., $I \propto \exp[-\kappa(S_0 + z)]$ changed to $\exp[-\kappa(S_0 + \Delta S + z)]$. Once the CO molecule on the Cu(111) surface was moved laterally, the CO-tip detected the tunnelling current from the substrate. The decay rate was obtained from the slopes of the I - z curves (see figure 2(d)). The decay rate changed before ($\kappa \sim 3.16$ Å⁻¹) and after ($\kappa \sim 2.47$ Å⁻¹) the CO lateral manipulation, i.e., the barrier height between the CO-tip and the CO molecule is $\phi \sim 9.49$ eV (see figure 2(e)): almost two times larger than the barrier height between the CO-tip and the bare Cu(111) surface, as shown in figure 1(g) (~ 4.97 eV). Such a large barrier height suppresses the electron tunnelling probability between tip and sample. Thus, electron-driven manipulation cannot be a major trigger for the CO-tip manipulation of the CO molecule. Although the W tip can cause the CO molecule to hop laterally on metal substrates by electron injection at ~ 50 mV [31–33], the CO-tip did not cause electron-driven hopping at 50 mV (see supplementary information, figure S2). This could be due to fewer electrons being injected from the CO-tip.

The DFT calculations in figure 2(c) support the above explanation of the experimental results shown in figure 2. The total energy of the CO molecules on the tip and substrate was calculated as a function of the distance between the tip and substrate. Previous AFM and DFT studies found three kinds of interactions between the CO-tip and CO molecules on substrates [15, 19, 20]: (1) short-range chemical interaction including Pauli repulsive interaction [19], (2) attractive van der

CO-tip \rightarrow CO-monomer

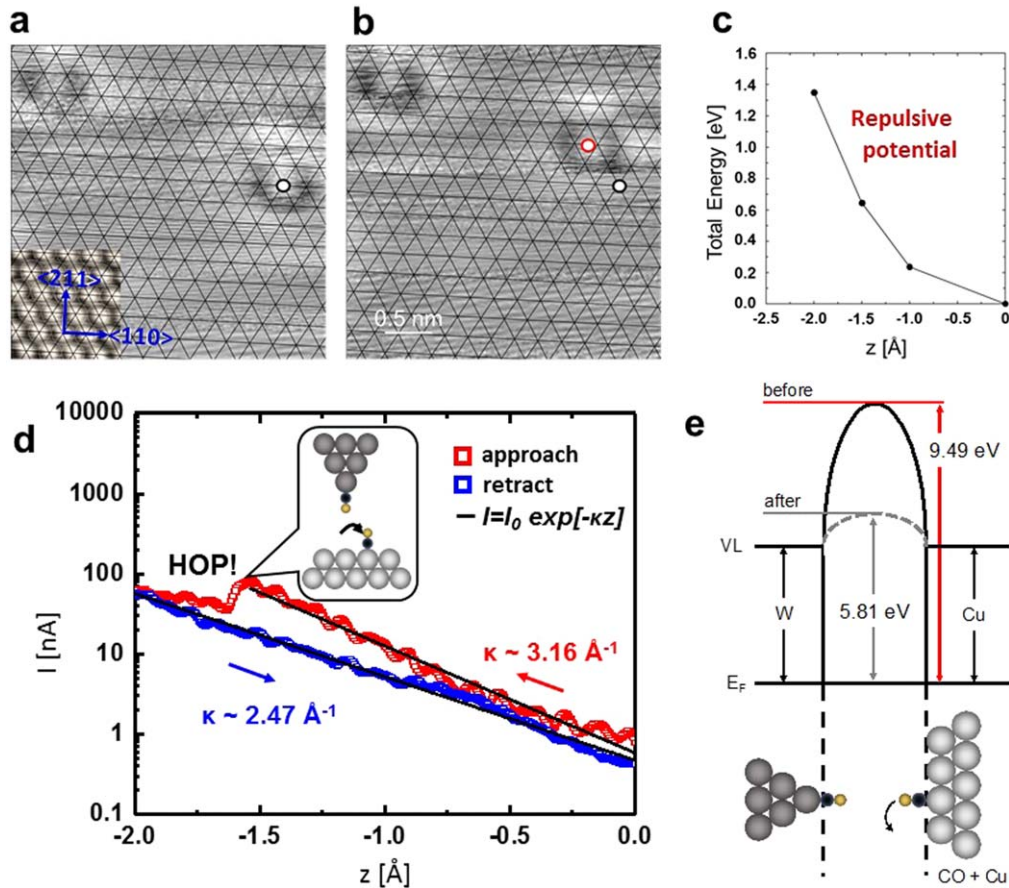


Figure 2. CO-tip manipulation of a CO-monomer. (a), (b) STM topography images of two single CO molecules adsorbed on Cu(111) obtained by the CO-tip ($V_s = +500$ mV, $I = 500$ pA). The overlaid black lines portray the Cu(111) fcc lattice as a guide for the eyes by using the Cu atomic image in the inset. In (a) the tip approached at the black circle position. In (b), the hopping CO is marked by a red circle. (c) Theoretical model and DFT calculation of the total energy of a system including a CO-tip. The total energy as a function of tip-sample distance shows the presence of repulsive interactions. Note that the total energy difference in this figure does not correspond to the energy barrier of the hopping of CO molecules. (d) $I-z$ spectroscopy curve. Blue-red squares were measured between (a) and (b). A lateral hopping event occurred at the current drop position. The decay rate (κ) was obtained by the least squares fitting of $I = I_0 \exp[-\kappa z]$ to the experimentally obtained $I-z$ data points: $\kappa = 3.157 \pm 0.024 \text{ \AA}^{-1}$ for approaching and $\kappa = 2.469 \pm 0.011 \text{ \AA}^{-1}$ for retracting. (e) Measured barrier height between the CO-tip and the CO monomer on Cu(111). Work function of Cu(111) (4.55 eV) and W(110) (4.80 eV) are shown [41]. E_F and VL denote the Fermi energy and vacuum level, respectively.

Waals (vdW) interaction at a larger tip-sample separation, and (3) the electrostatic dipole interaction by the CO molecules at a larger tip-sample separation [15, 19, 20]. Our DFT calculations include short-range force and electrostatic potential contribution. But vdW interaction is not included. It is difficult to distinguish the short-rang atomic force and the electrostatic potential from this calculation results itself. In what follows, we discuss which contribution is dominant in the CO molecule hopping event from the tip-sample separation.

In the STM measurement, the tip-sample separation, S , can be estimated from tunnelling resistance. The $I-z$ curves in figures 1–2 were measured at a typical setpoint of $V_s = 0.5$ V and $I = 0.5$ nA ($R = 10^9 \Omega$). When both the tip and sample are metal, $R = 10^9 \Omega$ corresponds to $S \sim 8 \text{ \AA}$. The tip-sample separation can be estimated as follows. Resistance at the

quantum point contact is $R = 12.9 \text{ k}\Omega \sim 10^4 \Omega$. At this point contact, the tip-sample separation corresponds to distance between the sample surface atom and the tip surface atom, i.e. $S \sim 3 \text{ \AA}$. One order of magnitude increase in the resistance roughly corresponds to an increase of the tip-sample separation by $\sim 1 \text{ \AA}$ ($R \propto \exp[\kappa S]$), thus the tip-sample separation at $R = 10^9 \Omega$ is simply estimated as $S \sim 3 + 5 = 8 \text{ \AA}$. However, the contact resistance increased from $10^4 \Omega$ to $R \sim 10^5 \Omega$ by using the CO-tip and the Cu(111) surface (see figure 1(f)). Therefore, the tip-sample separation at the typical setpoint decreased to $S \sim 3 + 4 = 7 \text{ \AA}$. Further, for the CO-tip and the target CO molecule case, the resistance just before the hopping was $R \sim 10^6 \Omega$ (see figure 2(d)). If we assume this is close to the contact, the tip-sample separation at the typical setpoint decreased to $S \sim 3 + 3 = 6 \text{ \AA}$. Since the hopping

event occurred by approaching the CO-tip 160 pm to the target CO molecule, the hopping event occurred at $S \sim 4.4 \text{ \AA}$. Although the short-range atomic force becomes dominant when tip-sample separation $< 300 \text{ pm}$ [19], at such a long-range regime, two interactions mainly exist: attractive vdW interaction and repulsive electrostatic dipole interaction. Thus, it is plausible that the long-range dipole–dipole repulsive interaction is the major trigger of the repulsive CO-tip manipulation.

In the CO-tip and the CO molecule on metal substrate case, both CO molecules have the same polarity. Although several possible dipole directions have been discussed in previous studies [15, 20, 34–36], these inconclusive arguments are beyond the scope of this study.

From the slope of the I - z curve during tip retraction ($z = -2 \text{ \AA}$ to 0 \AA) in figure 2(d), a barrier height of $\phi \sim 5.81 \text{ eV}$ was obtained (see figure 2(e)), which is $\sim 0.8 \text{ eV}$ higher than the barrier height of $\phi \sim 4.97 \text{ eV}$ between the CO-tip and the bare Cu(111). As discussed above, the CO lateral hopping event occurred at the tip-sample separation of $S \sim 4.4 \text{ \AA}$. When the CO hopped $\sim 5 \text{ \AA}$, the separation between two CO molecules increased to $S \sim 6.7 \text{ \AA}$. The experimentally obtained larger barrier height even after the hopping means that the CO-tip still experiences the repulsive force via the long-range dipole–dipole interaction. This could be also one evidence that the dipole–dipole repulsive interaction is the major trigger of the CO-tip manipulation.

CO-tip manipulation of CO-pair

The experimental and theoretical results in figure 2 tell us that the CO-tip is able to push the target CO molecule on a metal substrate with atomic-scale accuracy. Such a repulsive interaction could be due to dipole–dipole interactions between the two CO molecules. This type of delicate manipulation was further tested. As a target, we used the same CO molecule, but now another CO molecule was located at a distance of $\sim 0.5 \text{ nm}$ ($=2d$) away. If CO molecules on a Cu(111) surface have dipoles and the local surface potential is modified, we may see different behaviour when manipulating CO molecules with the CO-tip. Figure 3(a) shows four single CO molecules. Two molecules sit next each other (separated by a distance of $\sim 0.5 \text{ nm}$ ($=2d$)). We refer to these two molecules as a ‘pair’. The CO tip was brought to approach one CO in the pair; this is marked by a black triangle in figure 3(a). After the approach, we scanned the same area and obtained figure 3(b). The target molecule moved to a nearby atop-site position with a hopping distance of $2d$ along the $[\bar{1}10]$ direction. Notably, only the target molecule moved, while the other three molecules were not moved even though one of the three molecules was located only $\sim 0.5 \text{ nm}$ away from the target molecule. This is also strong evidence that the CO-tip can be used for highly accurate manipulation. Moreover, owing to the repulsive interaction between the CO molecules in the pair, the target CO molecule did not hop towards the neighbouring molecule. The stronger repulsive force for the pair was confirmed using the calculated electrostatic potentials in

figure 3(c), where CO molecules are located at the surface position ($z = 0$). In the vacuum region ($z > 1 \text{ \AA}$), the potential is constant, but it decays rapidly below the surface ($z < -0.5 \text{ \AA}$). A dip can be observed exactly at the surface CO position. The CO monomer (red line) and CO pair (blue line) have a potential dip of $\Delta E \sim 0.4 \text{ eV}$ and $\Delta E \sim 0.7 \text{ eV}$, respectively. The DFT calculation model is shown in supplementary information, figure S3. The larger ΔE of the pair indicates that the CO in the pair has a larger dipole, which could produce a large repulsive force against the CO-tip.

This interaction can be detected using the I - z curve (see figure 3(d)). The entire behaviour of the I - z curve is similar to that of the CO monomer case in figure 2. During the approach, first ($z = 0$ to -1.3 \AA), the tunnelling current exponentially increased. But, at $z \sim -1.3 \text{ \AA}$, a sudden drop in the current ($\sim 30 \text{ nA}$ down) was observed. Here, the target CO molecule below the CO-tip hopped laterally. Notably, the current drop was observed at a shorter tip displacement compared with the CO monomer case (the current drop at $z \sim -1.60 \text{ \AA}$ in figure 2(d)). This is strong experimental evidence that the CO-tip feels a stronger repulsive interaction for the CO pair case.

Similar to the interaction between the CO-tip and the CO monomer, shown in figure 3(d), before and after lateral hopping, the decay rate changed to $\kappa \sim 3.13 \text{ \AA}^{-1}$ while approaching and $\kappa \sim 2.53 \text{ \AA}^{-1}$ while retracting. That is, the barrier height between the CO-tip and the CO in the pair was $\sim 9.34 \text{ eV}$ (see figure 3(e)), while the barrier height between the CO-tip and the CO molecule after hopping was $\sim 6.07 \text{ eV}$ ($\sim 1 \text{ eV}$ higher than the barrier height between the CO-tip and the bare Cu(111) surface). The larger barrier height decreases the electron tunnelling probability. Therefore, CO manipulation by the CO-tip could be due to the repulsive force interaction rather than electron injection or excitation driven hopping.

Statistical analysis

In this section, we comment on the statistics of the hopping events. As observed in figures 2 and 3, the hopping distance, direction, and adsorption sites were not uniform. The energetically stable hopping position was investigated by repeating I - z measurements to obtain a statistical distribution. The hopping-distance histogram from when the CO-tip approached a CO monomer is shown in figure 4(a). Clearly, the nearest neighbour distance, $x = 1d = a/\sqrt{2} = 0.260 \text{ nm}$, is the energetically stable position: 55% of hops ended at $1d$, 21% at $2d$, 13% at $3d$, 5% at $4d$, and 5% at $5d$. This suggests that the CO-tip is capable of gentle manipulation at the atomic level. Vertical hopping was never observed. The experimentally obtained two-dimensional scattering map in figure 4(b) shows no clear directional dependence. The pushed CO monomers are located randomly. In figure 4(b), the centre position was the original position before scattering. Adsorption sites after hopping were also plotted (see supplementary information, figure S4(b)). Markedly, under this repulsive

CO-tip → CO-pair

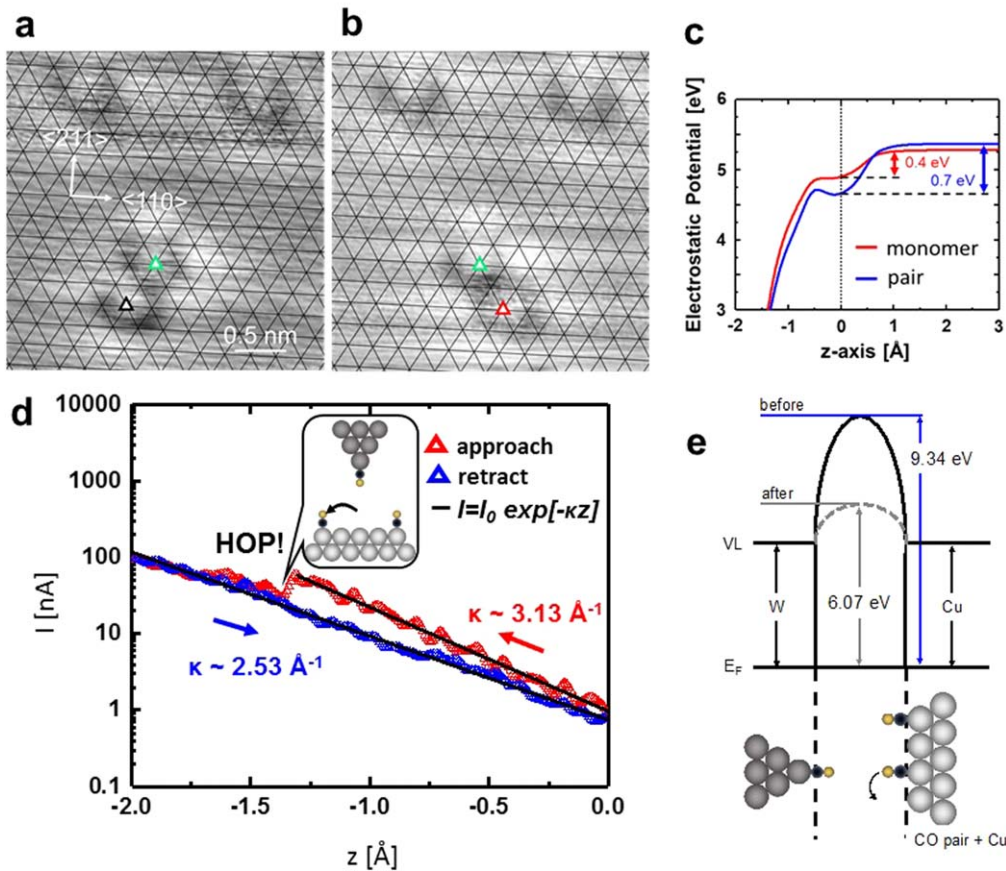


Figure 3. CO-tip manipulation of a CO-pair. (a), (b) STM topography images of four single CO molecules adsorbed on Cu(111) obtained by the CO-tip ($V_s = +500$ mV, $I = 500$ pA). The black lines denote the Cu(111) fcc lattices as a guide for the eyes. In (a) the tip approached at the black triangular position. After the hopping event in (b), only the CO molecule marked by the black triangular moved to the red triangular position. In (a) and (b), the CO molecule marked by the green triangle was not moved. (c) Calculated electrostatic potential for the CO monomer (red) and the CO pair (blue) adsorbed on Cu(111). (d) I - z spectroscopy curve. Blue-red triangles were measured between (a) and (b). The lateral hopping event occurred at the current drop position. The decay rate (κ) was obtained by the least squares fitting of $I = I_0 \exp[-\kappa z]$ to the experimentally obtained I - z data points: $\kappa = 3.133 \pm 0.026 \text{ \AA}^{-1}$ for approaching and $\kappa = 2.526 \pm 0.010 \text{ \AA}^{-1}$ for retracting. (e) Measured barrier height between the CO-tip and the CO pair on Cu(111). Work function of Cu(111) (4.55 eV) and W(110) (4.80 eV) are shown [41]. E_F and VL denote the Fermi energy and vacuum level, respectively.

manipulation, we observed that the atop site is the most preferred adsorption site, followed by bridge, hollow-hcp, and hollow-fcc sites. In other words, the closest atop site is energetically stable after hopping.

We note that the CO-tip successfully moved the target CO molecule with 72% chance (see supplementary information, figure S4(a)). The 28% failure rate can probably be attributed to the following factors. One is that the position actually approached is slightly shifted from the exact centre position of the CO molecule during tracking and targeting to poke the single CO molecule on the STM image. Another factor could be the tilting of the CO molecule on the W tip apex.

Statistical experiments clearly showed a difference between the CO monomer and the CO pair cases. The CO-tip was made to approach the target CO molecule in the pair. The obtained hopping-distance histogram is shown in figure 4(c).

The majority of the distances were found to be between $2d$ and $4d$ (23%–31%) instead of the nearest $1d$ (15%). The CO molecule in the pair prefers to hop more than two atomic distances from the initial position. Therefore, the CO-tip approaching the CO pair experienced a larger repulsive pushing force due to the neighbouring CO molecule. The scattering map is shown in figure 4(d). No clear directional dependence is observed.

Further, this stronger repulsive force for the pair case causes some randomness in the adsorption site after hopping. CO monomers prefer to hop to the atop site (see supplementary information, figure S4(b)), but for the CO-pair, bridge and atop sites are comparable; therefore, no clear site dependence is observed.

However, when the CO-tip approached the pair, manipulation was successful more than 90% of the time (see supplementary information, figure S4(a)). This experimental

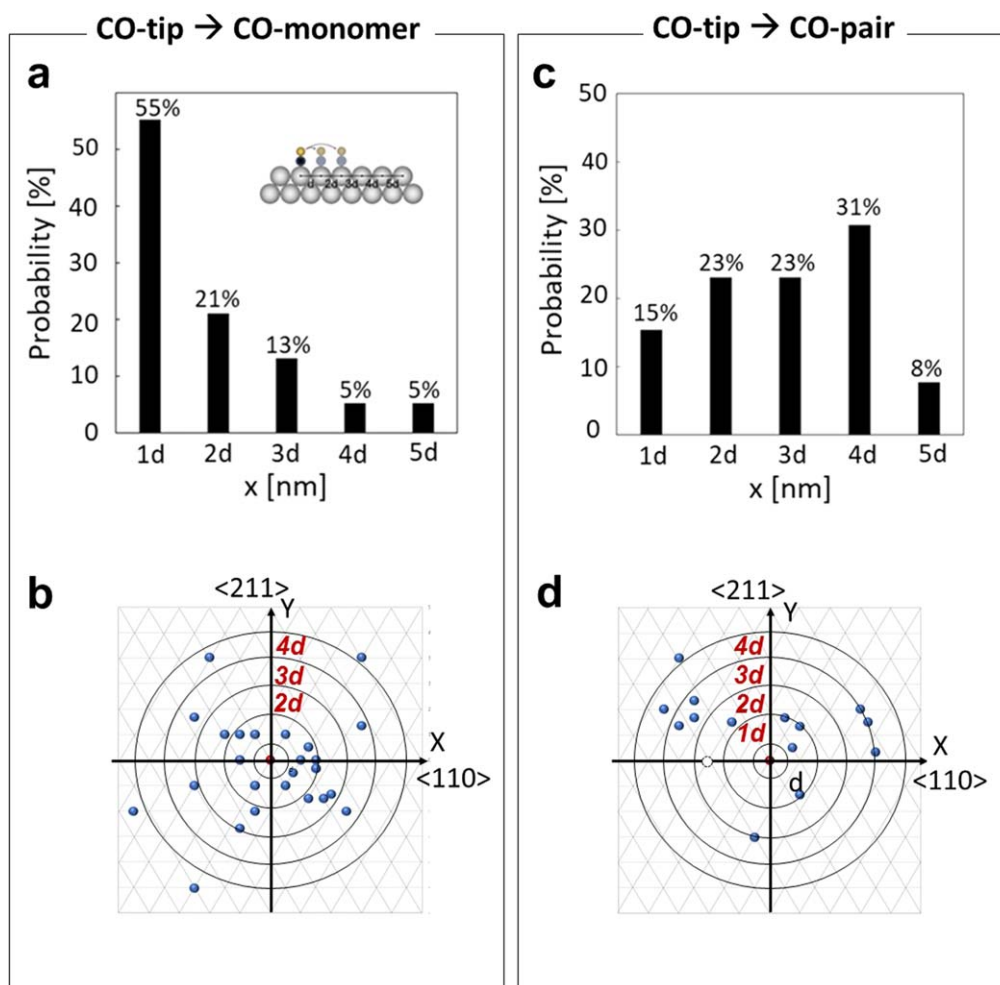


Figure 4. Statistical measurements obtained by repeating the lateral hopping events for (a), (b) CO-monomer and (c), (d) CO-pair cases. $1d$ corresponds to $a/\sqrt{2}$, 0.26 nm, where a denotes the Cu lattice constant. (a), (c) Hop distribution as a function of the distance measured from the original position. (b), (d) Two-dimensional X - Y plots of the hopped CO. X and Y axes are parallel to the $\langle 110 \rangle$ and $\langle 211 \rangle$ directions, respectively. The red dot shows the original position. The white dot shows the neighbouring CO in the pair.

evidence suggests stronger repulsive interactions for the CO pair case, which is likely due to dipole-dipole interactions.

Summary

We demonstrated repulsive lateral manipulation of CO molecules on a Cu(111) surface with atomic-scale accuracy by using the interactions between a CO/W-tip and the target CO molecule. Dipole-dipole interactions could be the key to this phenomenon. The CO-tip is able to precisely manipulate one target CO molecule without moving another CO located even at a distance of ~ 0.5 nm. Vertical hopping to the tip was never observed. All the STM experiments were performed in UHV at cryogenic temperature.

The lateral hopping event was directly monitored by simultaneously measuring the I - z curve. When the repulsive interaction overcomes the adsorption energy of CO on Cu(111), the target CO molecule was observed to hop laterally. This event was observed as a sudden current drop in

the I - z curve. From the exponential slope in the I - z curve, a large barrier height was measured between the CO-tip and the target CO molecule, which decreases the electron tunnelling probability between the tip and sample; therefore, electron-driven manipulation cannot be a major trigger for CO-CO repulsive manipulation. The CO on the tip apex was never observed to hop.

Statistical distributions of the lateral hopping distance of the target CO monomer after being approached by the CO-tip showed that the energetically stable position is the nearest neighbour atop site (~ 0.26 nm = $1d$). These statistical measurements also found that the CO-tip feels a larger repulsive interaction when the target CO molecule is part of a pair (two COs located next each other). In the pair case, the target CO hopped more than twice the distance without any site dependence.

This CO-tip repulsive manipulation technique can be useful for fabricating artificial two-dimensional CO molecule networks and CO molecular logic gates, or for achieving a better understanding of catalytic oxidation processes.

Experimental methods

Tip preparations

STM tips were fabricated from polycrystalline W wires with a radius of 0.3 μm (purity: 99.95%) using an electrochemical etching process, and subsequently transferred into UHV and cleaned using a tip-flashing process and checked using a field-emission technique [21]. The CO tip was fabricated by picking up a single CO molecule from the Cu(111) substrate onto a bare W tip in UHV at 5 K. Note that, in our study, CO molecules on the Cu(111) surface always shifted laterally, but the CO single molecule adsorbed on the W tip apex never moved, which was experimentally demonstrated as the CO molecules on Cu(111) were always observed as protrusions. This suggests that the CO π -orbital bonds more strongly with W 5d states than Cu 4s states.

I - z curve

The variation of the tunnelling current (I) as a function of the tip-apex displacement (z) was measured at a constant bias voltage. The zero position of the displacement ($z = 0$) was set as the initial position of the tip during the approach. The measured tip current was divided by the applied bias voltage, V_s , to calculate the conductance. The measured conductance was normalised by $G_0 = 2e^2/h$, where e is the electron mass and h is Planck's constant. The I - z method requires the feedback to be turned off, and the tip was gradually moved toward the target molecule precisely [37].

Sample preparations

The Cu(111) surface was cleaned using repeated cycles of Ar^+ sputtering (+1.0 kV, +0.80 μA) for 15–30 min with subsequent annealing (~ 820 K). The cleanliness of the substrate was verified using low-energy electron diffraction. After cleaning, the Cu(111) substrate was left to cool for 30 min, and thereafter placed on a pre-cooling stage (100 K) for 15 min before insertion into the STM stage. The Cu(111) substrate was thereafter left to cool to 5 K on the STM stage for at least 3 h. Before depositing CO molecules, the surface was examined using STM and spectroscopy measurement (supplementary information, figure S5). In most cases, immediately after cleaning the surface, terraces of >100 nm were produced with impurity concentrations of $<1\%$ (see figures S5(a), (b), (d)). From differential conductance (dI/dV) spectra measurements, the surface state peak of Cu(111) could be observed at -0.35 eV below the Fermi energy, E_F (see figure S5(c)). After confirming the state of the Cu(111) surface, CO single molecules were adsorbed onto the surface. The STM chamber was exposed to 0.1 L ($1 \text{ L} = 1.33 \times 10^{-6}$ mbar s) of CO gas (purity 99.9%) from a variable leak valve (see supplementary information, figure S6). During the exposure (100 s at 10^{-7} Pa), the shield covering the STM was opened, which caused the substrate temperature to increase slightly (~ 10 K, base temperature 5 K).

Theoretical calculations

DFT calculations were performed using the Vienna *ab initio* simulation package [38, 39] with the projected augmented wave method [40]. The cutoff energy for the plane wave expansion was set to 400 eV. The exchange and correlation were described at the level of the generalised gradient approximation. For the calculation including the STM tip, we modelled the Cu(111) surface with the STM tip using a 10-layer thickness slab model with a (2×2) supercell where an additional Cu atom representing the STM tip was placed at the bottom surface. The distance between the tip and surface was controlled by changing the lattice constant of the z -axis. The atomic positions were optimised until the forces on the respective atoms were less than 0.01 eV \AA^{-1} . The Brillouin zone was sampled using a $7 \times 7 \times 1$ Monkhorst–Pack k -mesh. The atoms in the bottommost Cu layer and the additional Cu atom were fixed during the optimisation. For the calculation of the electrostatic potential, the Cu(111) surface was modelled with a five-layer thickness slab model with a (7×7) supercell. Owing to the large dimensions of the supercell, the Brillouin zone was sampled with a single k -point only at the Γ point. In all cases, we used the hollow site as the stable adsorption site of CO.

Acknowledgments

This work was supported by JSPS KAKENHI Grant Nos. 23681018, 25110011 and the Asahi Glass Foundation. We thank to Dr Eiichi Inami for valuable discussions. Dr Naoka Ohta provided support for experiments of $\text{H}_2\text{Pc}/\text{Cu}(111)$ with the CO-tip.

ORCID iDs

T K Yamada  <https://orcid.org/0000-0001-5185-6472>

References

- [1] Komeda T, Kim Y, Kawai M, Persson B N J and Ueba H 2002 Lateral hopping of molecules induced by excitation of internal vibration mode *Science* **295** 2055–8
- [2] Heinrich A J, Lutz C P, Gupta J A and Eigler D M 2002 Molecule cascades *Science* **298** 1381–7
- [3] Gomes K K, Mar W, Ko W, Guinea F and Manoharan H C 2012 Designer Dirac fermions and topological phases in molecular graphene *Nature* **483** 306–10
- [4] Bartels L, Meyer G, Rieder K-H, Velic D, Knoesel E, Hotzel A, Wolf M and Ertl G 1998 Dynamics of electron-induced manipulation of individual CO molecules on Cu(111) *Phys. Rev. Lett.* **80** 2004–7
- [5] Welker J and Giessibl F J 2012 Revealing the angular symmetry of chemical bonds by atomic force microscopy *Science* **336** 444–9
- [6] Bartels L, Meyer G and Rieder K-H 1997 Controlled vertical manipulation of single CO molecules with the scanning tunneling microscope: a route to chemical contrast *Appl. Phys. Lett.* **71** 2

- [7] Wintterlin J, Volkeneing S, Janssens T V W, Zambelli T and Ertl G 1997 Atomic and macroscopic reaction rates of a surface-catalyzed reaction *Science* **278** 1931
- [8] Hahn J R and Ho W 2001 Oxidation of a single carbon monoxide molecule manipulated and induced with a scanning tunneling microscope *Phys. Rev. Lett.* **87** 166102
- [9] Bonn M, Funk S, Hess C, Denzler D N, Stampß C, Scheffßer M, Wolf M and Ertl G 1999 Phonon-versus electron-mediated desorption and oxidation of CO on Ru(0001) *Science* **285** 1042
- [10] Slot M R, Gardenier T S, Jacobse P H, van Miert G C P, Kempkes S N, Zevenhuizen S J M, Smith C M, Vanmaekelbergh D and Swart I 2017 Experimental realization and characterization of an electronic Lieb lattice *Nat. Phys.* **13** 672
- [11] Drost R, Ojanen T, Harju A and Liljeroth P 2017 Topological states in engineered atomic lattices *Nat. Phys.* **13** 668
- [12] Collins L C, Witte T G, Silverman R, Green D B and Gomes K K 2017 Imaging quasiperiodic electronic states in a synthetic Penrose tiling *Nat. Commun.* **8** 15961
- [13] Emmrich M, Schneiderbauer M, Huber F, Weymouth A J, Okabayashi N and Giessibl F J 2015 Force field analysis suggests a lowering of diffusion barriers in atomic manipulation due to presence of STM tip *Phys. Rev. Lett.* **114** 146101
- [14] Gross L, Mohn F, Moll N, Liljeroth P and Meyer G 2009 The chemical structure of a molecule resolved by atomic force microscopy *Science* **325** 1110–4
- [15] Ellner M, Pavlicek N, Pou P, Schuler B, Moll N, Meyer G, Gross L and Perez R 2016 The electric field of CO tips and its relevance for atomic force microscopy *Nano Lett.* **16** 1974–80
- [16] Moll N, Gross L, Mohn F, Curioni A and Meyer G 2010 The mechanisms underlying the enhanced resolution of atomic force microscopy with functionalized tips *New J. Phys.* **12** 125020
- [17] Sweetman A, Rashid M A, Jarvis S P, Dunn J L, Rahe P and Moriarty P 2016 Visualizing the orientational dependence of an intermolecular potential *Nat. Commun.* **7** 10621
- [18] Weymouth A J, Hofmann T and Giessibl F J 2014 Quantifying molecular stiffness and interaction with lateral force microscopy *Science* **343** 1120–2
- [19] Sun Z, Boneschanscher M P, Swart I, Vanmaekelbergh D and Liljeroth P 2011 Quantitative atomic force microscopy with carbon monoxide terminated tips *Phys. Rev. Lett.* **106** 046104
- [20] Swaraz A, Kohler A, Grenz J and Weisendanger R 2014 Detecting the dipole moment of a single carbon monoxide molecule *Appl. Phys. Lett.* **105** 011606
- [21] Yamada T K, Abe T, Nazriq N K M and Irisawa T 2016 Electron-bombarded (110)-oriented tungsten tips for stable tunneling electron emission *Rev. Sci. Instrum.* **87** 033703
- [22] Bartels L, Meyer G and Rieder K-H 1999 The evolution of CO adsorption on Cu(111) as studied with bare and CO-functionalized scanning tunneling tips *Surf. Sci.* **432** 621–6
- [23] Blyholder G 1964 Molecular orbital view of chemisorbed carbon monoxide *J. Phys. Chem.* **68** 2772
- [24] Lauhon L J and Ho W 1999 Single-molecule vibrational spectroscopy and microscopy: CO on Cu(001) and Cu(110) *Phys. Rev. B* **60** R8525
- [25] Fielicke A, Gruene P, Meijer G and Rayner D M 2009 The adsorption of CO on transition metal clusters: a case study of cluster surface chemistry *Surf. Sci.* **603** 1427–33
- [26] Zhang R, Hu Z, Li B and Yang J 2014 Efficient method for fast simulation of scanning tunneling microscopy with a tip effect *J. Phys. Chem. A* **118** 8953–9
- [27] Drakova D, Nedjalkova M and Doyen G 2006 Theory of tip-dependent imaging of adsorbates in the STM: CO on Cu(111) *Int. J. Quantum Chem.* **106** 1419–31
- [28] Aizawa H and Tsuneyuki S 1997 First-principles study of CO bonding to Pt(111): validity of the Blyholder model *Surf. Sci.* **399** L364–70
- [29] Vitali L, Ohmann R, Kern K, Garcia-Lekue A, Frederiksen T, Sanchez-Portal D and Arnau A 2010 Surveying molecular vibrations during the formation of metal-molecule nanocontacts *Nano Lett.* **10** 657
- [30] Yamada T K, Fujii J and Mizoguchi T 2001 STM, STS, and local work function study of Cs/p-GaAs (110) *Surf. Sci.* **479** 33–42
- [31] Uvdal P, Karlsson P-A, Nyberg C, Andersson S and Richardson N V 1988 On the structure of dense CO overlayers *Surf. Sci.* **202** 167–82
- [32] Froitzheim H, Ibach H and Lehwald S 1977 Surface vibrations of CO on W(100) *Surf. Sci.* **63** 56–66
- [33] Held G, Schuler J, Sklarek W and Steinrück H-P 1998 Determination of adsorption sites of pure and coadsorbed CO on Ni(111) by high resolution x-ray photoelectron spectroscopy *Surf. Sci.* **398** 154–71
- [34] Hapala P, Kichin G, Wagner C, Tautz S, Temirov R and Jelinek P 2014 Mechanism of high-resolution STM/AFM imaging with functionalized tips *Phys. Rev. B* **90** 085421
- [35] Hapala P, Temirov R, Tautz S and Jelinek P 2014 Origin of high-resolution IETS-STM images of organic molecules with functionalized tips *Phys. Rev. Lett.* **113** 226101
- [36] Hoffman T, Pielmeier F and Giessibl F J 2014 Chemical and crystallographic characterization of the tip apex in scanning probe microscopy *Phys. Rev. Lett.* **112** 066101
- [37] Kitaguchi Y, Habuka S, Okuyama H, Hatta S, Aruga T, Frederiksen T, Paulsson M and Ueba H 2015 Controlled switching of single-molecule junctions by mechanical motion of a phenyl ring *Beil. J. Nanotechnol.* **6** 2088–95
- [38] Kresse G and Furthmüller J 1996 Efficient iterative schemes for *ab initio* total-energy calculations using plane-wave basis set *Phys. Rev. B* **54** 11169–86
- [39] Kresse G and Furthmüller J 1996 Efficiency of *ab-initio* total energy calculations for metals and semiconductors using a plane-wave basis set *Comput. Mater. Sci.* **6** 15–50
- [40] Blöchl P E 1994 Projector augmented-wave method *Phys. Rev. B* **50** 17953–79
- [41] Miedema A R, Chatel P F and Boer F R 1980 Cohesion in alloys—fundamentals of semi-empirical model *Physica* **100B** 1–28